

A dynamic soil chamber system coupled with a tunable diode laser for online measurements of $\delta^{13}\text{C}$, $\delta^{18}\text{O}$, and efflux rate of soil-respired CO_2 [†]

Heath H. Powers^{1*}, John E. Hunt², David T. Hanson³ and Nate G. McDowell¹

¹Earth and Environmental Sciences Division, MS-J495, Los Alamos National Laboratory, Los Alamos, NM 87544, USA

²Landcare Research, P.O. Box 40, Lincoln 7640, New Zealand

³Department of Biology, University of New Mexico, 167 Castetter Hall, Albuquerque, NM 87131, USA

Received 16 September 2009; Revised 7 November 2009; Accepted 11 November 2009

High frequency observations of the stable isotopic composition of CO_2 effluxes from soil have been sparse due in part to measurement challenges. We have developed an open-system method that utilizes a flow-through chamber coupled to a tunable diode laser (TDL) to quantify the rate of soil CO_2 efflux and its $\delta^{13}\text{C}$ and $\delta^{18}\text{O}$ values ($\delta^{13}\text{C}_\text{R}$ and $\delta^{18}\text{O}_\text{R}$, respectively). We tested the method first in the laboratory using an artificial soil test column and then in a semi-arid woodland. We found that the CO_2 efflux rates of 1.2 to 7.3 $\mu\text{mol m}^{-2} \text{s}^{-1}$ measured by the chamber-TDL system were similar to measurements made using the chamber and an infrared gas analyzer (IRGA) ($R^2 = 0.99$) and compared well with efflux rates generated from the soil test column ($R^2 = 0.94$). Measured $\delta^{13}\text{C}$ and $\delta^{18}\text{O}$ values of CO_2 efflux using the chamber-TDL system at 2 min intervals were not significantly different from source air values across all efflux rates after accounting for diffusive enrichment. Field measurements during drought demonstrated a strong dependency of CO_2 efflux and isotopic composition on soil water content. Addition of water to the soil beneath the chamber resulted in average changes of +6.9 $\mu\text{mol m}^{-2} \text{s}^{-1}$, -5.0‰ , and -55.0‰ for soil CO_2 efflux, $\delta^{13}\text{C}_\text{R}$ and $\delta^{18}\text{O}_\text{R}$, respectively. All three variables initiated responses within 2 min of water addition, with peak responses observed within 10 min for isotopes and 20 min for efflux. The observed $\delta^{18}\text{O}_\text{R}$ was more enriched than predicted from temperature-dependent $\text{H}_2\text{O}-\text{CO}_2$ equilibration theory, similar to other recent observations of $\delta^{18}\text{O}_\text{R}$ from dry soils (Wingate L, Seibt U, Maseyk K, Ogee J, Almeida P, Yakir D, Pereira JS, Mencuccini M. *Global Change Biol.* 2008; 14: 2178). The soil chamber coupled with the TDL was found to be an effective method for capturing soil CO_2 efflux and its stable isotope composition at high temporal frequency. Published in 2010 by John Wiley & Sons, Ltd.

The carbon and oxygen isotopic compositions of atmospheric CO_2 ($\delta^{13}\text{C}$ and $\delta^{18}\text{O}$, respectively) reflect fractionation by terrestrial ecosystems,¹ providing a valuable tracer of biosphere-atmosphere CO_2 exchange.^{2–4} The isotopic composition of soil respiration ($\delta^{13}\text{C}_\text{R}$ and $\delta^{18}\text{O}_\text{R}$) has a large impact on atmospheric $\delta^{13}\text{C}$ and $\delta^{18}\text{O}$ because it is among the largest CO_2 fluxes to the atmosphere. Approximately 68 Gt of CO_2 per year evolves from the soil,⁵ more than 10 times the amount emitted through fossil fuel combustion.⁶ Soil-respired $\delta^{13}\text{C}$ ($\delta^{13}\text{C}_\text{R}$) reflects microbial and root respiration of photosynthetic products,^{7,8} while soil-respired $\delta^{18}\text{O}$ ($\delta^{18}\text{O}_\text{R}$) approximately reflects the $\delta^{18}\text{O}$ of soil water.^{9,10} Models of ecosystem and global carbon cycles based on constant values of terrestrial isotopic fractionation during respiration may give incorrect results if the isotopic

composition of terrestrial respiration is incorrectly parameterized.^{11,12} This problem stems from a lack of data on $\delta^{13}\text{C}_\text{R}$ and $\delta^{18}\text{O}_\text{R}$.

Although major advances in our knowledge have occurred in recent decades, the mechanisms regulating $\delta^{13}\text{C}_\text{R}$ and $\delta^{18}\text{O}_\text{R}$ (δ_R collectively) remain poorly understood.^{9,13,14} For example, soil metabolism responds rapidly to pulse events such as rainfall,¹⁵ but observations of this response are rarely quantified due to technical limitations associated with the tedious and expensive process of flask collection and analyses via traditional mass spectrometry techniques. In the existing studies on soil-respired $\delta^{13}\text{C}$ and $\delta^{18}\text{O}$, several chamber types were used but all involved periodically collecting gas samples and taking them for post-analysis by mass spectrometry^{16–18} (but see recent exceptions^{19,20}). In these experiments, the frequency of sample collection was inherently limited by the time and effort required for flask collection and offline mass spectrometric analysis. A relatively new technique, commonly referred to as tunable diode laser (TDL) spectroscopy, overcomes these challenges. TDL spectroscopy uses a laser with an emission frequency

*Correspondence to: H. H. Powers, Earth and Environmental Sciences Division, MS-J495, Los Alamos National Laboratory, Los Alamos, NM 87544, USA.

E-mail: hpowers@lanl.gov

[†]This article is a U.S. Government work and is in the public domain in the U.S.A.

that can be varied to match the absorption frequency of specific isotopologues and scan the breadth of the absorbance feature.²¹ This is done for all of the isotopologues of interest (e.g. $^{13}\text{C}^{16}\text{O}_2$, $^{12}\text{C}^{16}\text{O}_2$, $^{12}\text{C}^{18}\text{O}^{16}\text{O}$) with high frequency so mole fractions of each species can be quantified. The particular instrument used in this study (TGA100A, Campbell Scientific, Logan, UT, USA) has a scan rate of 500 Hz with data output averaged to 10 Hz for high-frequency measurements, although typically measurements are averaged for 10–15 s for improved precision. TDL measurements have become increasingly important in isotopic studies because they allow large numbers of measurements to be collected continuously.^{20–23} For example, pulse responses to precipitation occur within minutes but the δ_R response has rarely been documented.^{16,24} Isotopic soil CO_2 efflux studies thus far have greatly benefited from the application of high-frequency measurements.^{19,20}

An additional complication for quantifying soil-respired isotopes is that chamber-based samples are difficult to collect without adversely affecting the rate of soil efflux and its isotopic composition.^{25–27} This problem can exist for all types of dynamic soil respiration systems. These chamber systems can create pressure differentials between the inside and outside of the chamber due to air being blown or drawn through the chamber resulting in advection rather than natural diffusion of CO_2 from the soil pore space into the chamber.^{28,29} Differences in pressure of as little as 1 Pa have been shown to affect efflux measurements by inducing mass flow of CO_2 either into or out of the soil. Ideally, pressure differences of less than 0.1 Pa are required for accurate measurements.³⁰ Closed systems, which have an opening to the soil but are otherwise closed to the atmosphere (see Norman *et al.*³¹), have an additional pressure perturbation to the soil surface: removing a gas sample for isotopic analysis from the otherwise constant-volume system creates a pressure reduction in the chamber that can result in mass flow of soil gas into the chamber headspace.³²

For isotopic measurements, open systems have an advantage over closed systems in that subsamples can be collected from the open chamber inlet and exhaust without altering the pressure inside the chamber, thereby averting mass air flow from the soil pore space that biases efflux and δ_R values. Open or flow-through soil chambers have a continuous flow of air through the chamber headspace, an inlet for incoming air, an outlet for exhausting air, and an opening to the soil surface. By using the 'online' approach of Evans *et al.*,³³ the CO_2 efflux rate and δ_R are calculated from differences in the chamber inlet and exhaust $[\text{CO}_2]$ and isotopic values. This technique lends itself well to high-frequency analysis by subsampling the open chamber inlet and exhaust in real time with TDL spectroscopy.

We explored the use of a TDL coupled to a dynamic flow-through chamber system modified from Fang and Moncrieff³⁰ for measuring soil CO_2 efflux, $\delta^{13}\text{C}_R$ and $\delta^{18}\text{O}_R$ at high temporal frequency. We used a TDL to sample the inlet and outlet of the chamber in order to produce these measurements at 2 min intervals, a frequency that we hypothesized was sufficient to capture rapid, transient shifts in respiration and δ_R values. We assessed the accuracy and precision of this system using an artificial soil test column with known efflux

rates and isotopic composition. In addition, we field-tested the chamber to determine the ability of the system to capture dynamic, transient events associated with pulse wetting of soils.

EXPERIMENTAL

Theory

Soil CO_2 efflux strongly controls near-surface atmospheric $[\text{CO}_2]$ and its stable isotopic composition due to the high $[\text{CO}_2]$ and large surface area of soils. Kinetic fractionation causes changes in the $\delta^{13}\text{C}$ and $\delta^{18}\text{O}$ of CO_2 within the pore space of the soil matrix relative to the source emitting the CO_2 .³⁴ This fractionation is estimated to be up to 4.4‰ for $\delta^{13}\text{C}$ and 8.8‰ for $\delta^{18}\text{O}$.^{18,34} Under steady-state conditions, CO_2 within the soil pore space is isotopically enriched relative to source values while gas leaving the soil surface has the same isotopic composition as the source emitting CO_2 into the soil.³⁵ Liquid water in soils affects the $\delta^{18}\text{O}$ value of respired CO_2 because CO_2 and water exchange oxygen atoms, thus imparting the water $\delta^{18}\text{O}$ signature onto the CO_2 with a temperature-dependent equilibrium fractionation.^{36–38} Net soil CO_2 efflux can be determined by the mass balance equation modified from Ball:³⁹

$$r = \frac{u_o(c_i - c_o)}{s} \quad (1)$$

where r is the net soil CO_2 efflux ($\mu\text{mol CO}_2 \text{ m}^{-2} \text{ s}^{-1}$), u_o is the flow rate out of the chamber ($\mu\text{mol s}^{-1}$), c_i is the mole fraction of CO_2 entering the chamber ($\mu\text{mol mol}^{-1}$), c_o is the mole fraction of CO_2 exiting the chamber ($\mu\text{mol mol}^{-1}$), and s is the surface area within the chamber (m^2).

A mass balance equation is used to determine $\delta^{13}\text{C}_R$ and $\delta^{18}\text{O}_R$ based on the difference in inlet and outlet δ values. The equation below was originally used for a respiring leaf in an open chamber and has been modified from Evans *et al.*³³ to apply it to an open soil chamber:

$$\delta_R = \frac{c_o\delta_o - c_i\delta_i}{c_o - c_i} \quad (2)$$

where δ_R is the isotopic value of CO_2 respired from the soil relative to the isotopic standards Vienna Pee Dee Belemnite (VPDB) for $\delta^{13}\text{C}$ and Vienna Standard Mean Ocean Water (VSMOW) for $\delta^{18}\text{O}$, δ_o is the delta value of air exiting the chamber outlet and δ_i is the delta value of air entering the chamber inlet.

Chamber design

The soil chamber used in this study is a dynamic flow-through chamber modified from Fang and Moncrieff.³⁰ The chamber was constructed from 3 mm polycarbonate and was rectangular with an internal volume of 2.65 L (Fig. 1). The inlet and outlet are located on either side of the chamber with a metal mesh placed in front of both the inlet and the outlet to help attenuate pressure waves from crossing the chamber. A slowly turning three-bladed fan (18 rpm) was used in the top of the chamber above the soil gas inlet to aid in mixing. The chamber bottom was circular with a diameter of 142 mm and a surface area of $15.8 \times 10^{-3} \text{ m}^2$. The bottom edge of the chamber protruded 30 mm from the lower surface and fitted into a water-sealed metal soil collar that was driven into the

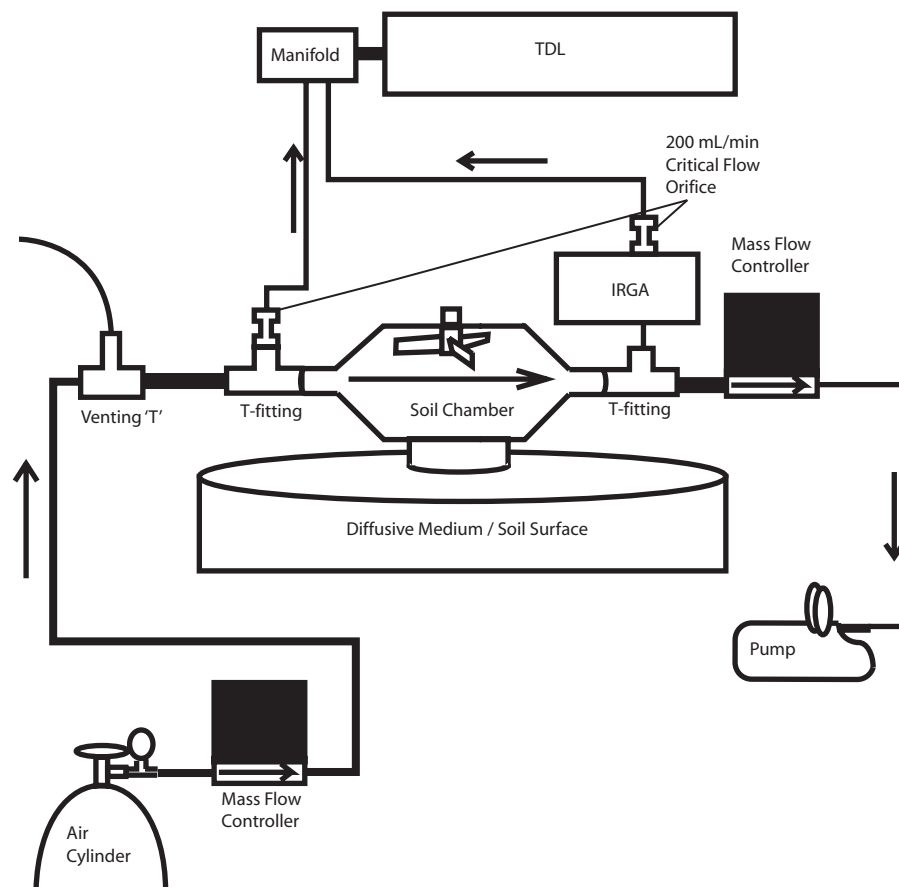


Figure 1. Schematic of the plumbing of the *TDL*-soil respiration chamber system used in this study. Flow from a compressed air cylinder is controlled by a mass flow controller and a tee that acts as a pressure bypass. The air is subsampled by the *TDL* before and after it enters the chamber. An additional mass flow controller regulates the flow out of the chamber to the pump. See Experimental section for further details.

soil or test column medium. The water seal prevents gas leakage while not influencing the $\delta^{18}\text{O}_\text{R}$ measurements because the exposure of liquid water to air in the chamber is less than 0.1% of the interior surface area (see results for accuracy of $\delta^{18}\text{O}_\text{R}$ measurements). The chamber was equipped with a thermocouple for measuring chamber headspace temperature, a port with an attached tube for connection to a differential pressure transducer, and a circular, perforated manifold placed over the bottom opening attached to an external tube for water delivery (watering experiments only).

The flow rate through the chamber was controlled with a mass flow controller (FMA-A2408, Omega Engineering, Stamford, CT, USA) connected to a diaphragm vacuum pump and attached to the chamber outlet in order to draw gas through the chamber. In order to minimize pressure differentials induced by restriction of the chamber inlet, a compressed gas cylinder of medical-grade air was attached to the chamber inlet and its flow was regulated with a mass flow controller in order to balance it with the rate at which air was drawn from the chamber (Fig. 1). The numerous medical-grade air cylinders used throughout the experiment had similar $[\text{CO}_2]$ and isotopic values to atmospheric air ($[\text{CO}_2] \approx 400$ ppm, $\delta^{13}\text{C} \approx -8.5\text{‰}$, $\delta^{18}\text{O} \approx 30\text{‰}$), minimizing

lateral diffusion in the soil associated with differences between air flowing over the soil surface inside and outside the chamber.²⁶ Using cylinder air rather than buffered ambient air provided enhanced isotopic and mole fraction stability of incoming air, increasing the precision of the measurement system by limiting the concentration and isotopic fluctuations used to calculate δ_R (Eqn. (2)) to the chamber outlet (see sensitivity calculation in Results section).

Prior to all measurements, the bottom of the chamber was sealed with closed-cell foam and the chamber flow rate was set with the outlet flow controller to the desired flow-through rate (between 0.3 and 1 L min^{-1} , depending on the experiment). A differential pressure transducer (PX653, Omega Engineering) was connected to measure the pressure difference between the inside and outside of the chamber. The flow rate from the air cylinder was then adjusted in order to bring the pressure differential to within ± 0.05 Pa, the resolution limit of the pressure transducer. After balancing the pressure of the chamber, the foam was removed and the chamber was placed on the collar for measurements.

Tee fittings (Fig. 1) were placed at both the chamber inlet and the outlet to allow subsampling by the *TDL* and an infrared gas analyzer (IRGA, LI-840, LI-COR Biosciences, Lincoln, NE, USA) for determination of chamber CO_2 efflux

and δ_R . Gas from the outlet tee was first routed through the IRGA for $[\text{CO}_2]$ analysis, then through a critical flow orifice (restricting flow to 200 mL min^{-1}) and into the TDL for $[\text{CO}_2]$, $\delta^{13}\text{C}$, and $\delta^{18}\text{O}$ analysis before being exhausted by the vacuum pump. The venting tee (Fig. 1) is used to maintain the pressure of the soil chamber at atmospheric pressure.

Soil test column

A soil test column was designed to mimic a soil emitting CO_2 from its surface for the purpose of testing the soil chamber response to known CO_2 efflux rates and isotopic composition. The cylindrical column was constructed of aluminum with a diameter of 1 m and height of 1.3 m. The bottom was sealed with sheet aluminum and the top had a perforated stainless steel grate (holes are 3.2 mm in diameter, 22.3 holes per cm^2) fitted 10 cm from the top edge. A porous nylon fabric was placed on top of the grate and held an 8 mm thick layer of the diffusive medium (3 mm diameter glass beads). The interior CO_2 delivery manifold was made from a 1.5 m length of copper tubing (1.3 mm i.d.) with small perforations approximately 60 mm apart, and placed in the bottom of the column. A similar manifold was constructed but of 0.4 m in length for monitoring CO_2 in the hollow volume beneath the diffusive medium with an IRGA (LI-820, LI-COR Biosciences) in a closed loop. A slowly rotating mixer (12 rpm) was placed in the bottom of the column above the CO_2 delivery manifold to aid in homogenizing the air within the test column.

Efflux from the test column was generated by raising the $[\text{CO}_2]$ in the hollow volume below the diffusive medium to create a CO_2 diffusion gradient between the interior of the column and the ambient air above the column. Constant CO_2 efflux rates from the test column were generated by maintaining constant $[\text{CO}_2]$ below the diffusive medium inside the column as monitored with an IRGA; the efflux was determined by measuring the amount of CO_2 gas that was emitted into the volume of the column in order to maintain a steady $[\text{CO}_2]$. This approach should avoid errors associated with mass flow caused when CO_2 is pumped into the column since it only replaced diffusive loss of CO_2 through surface efflux.^{29,40} A mass flow controller (FMA-2402, Omega Engineering, 20 mL min^{-1} maximum) was used to regulate the flow of CO_2 into the column volume. The CO_2 was from a compressed cylinder of 99.9% CO_2 ($\delta^{13}\text{C} = -41.3\text{‰}$, $\delta^{18}\text{O} = 3.8\text{‰}$). A data logger (CR1000, Campbell Scientific) was programmed with a feedback algorithm that regulated the delivery of CO_2 into the test column (via the mass flow controller) in order to maintain a target CO_2 concentration inside the column. Commands were sent to the mass flow controller every second and flow data was recorded and averaged over 5 min intervals to determine the surface CO_2 efflux rates of the test column. Measurements were conducted once the column reached steady state as determined by the standard deviation of CO_2 efflux from the column being within $\pm 0.05 \mu\text{mol CO}_2 \text{ m}^{-2} \text{ s}^{-1}$ over the course of 1 h. Gradients of $[\text{CO}_2]$ from below to above the glass beads during the experiment ranged from 700 to $4500 \mu\text{mol mol}^{-1}$.

To determine $\delta^{13}\text{C}_R$ and $\delta^{18}\text{O}_R$ from test column efflux, TDL measurements were made on the CO_2 within the hollow

volume of the test column beneath the diffusive medium. In order to bring a gas sample of suitable concentration for TDL sampling, mass flow controllers were used to mix the gas with CO_2 -free air to produce a sample stream with a $[\text{CO}_2]$ of $\sim 400 \mu\text{mol mol}^{-1}$. The CO_2 within the volume of the test column was assumed to be isotopically enriched due to kinetic fractionation at steady state³⁵ and the measured values were converted into δ_R values by subtracting 4.4‰ for $\delta^{13}\text{C}$ and 8.8‰ for $\delta^{18}\text{O}$, giving known values for surface efflux CO_2 of $\delta^{13}\text{C}_R = -39.0 \pm 0.3\text{‰}$ and $\delta^{18}\text{O}_R = 9.7 \pm 0.3\text{‰}$.

Soil chamber operation

Prior to testing, a soil collar was placed into the diffusive medium of the test column, the top of the column was sealed with a lid and all of the CO_2 was removed using a soda lime scrubber. Testing began by first bringing the interior air of the test column to a steady-state target $[\text{CO}_2]$ as determined by the IRGA. The chamber was then placed on the collar for efflux measurement and the flow rate through the chamber was chosen as either 300 or 500 mL min^{-1} . These rates were chosen to optimize the chamber headspace $[\text{CO}_2]$ by maximizing the difference between c_o and c_i but remaining within the calibrated range of the TDL. Chamber measurements of $[\text{CO}_2]$ were made using both the TDL and the independent IRGA for comparison of the TDL-based measurement with the traditional IRGA-based measurement. Since the IRGA only measured the chamber outlet, a predetermined value for $[\text{CO}_2]$ from the medical-grade air cylinder was used as the inlet value in IRGA-based efflux calculations. Chamber measurements of the test column were conducted at multiple column CO_2 efflux rates. The test column was allowed to equilibrate at each efflux rate for a minimum of 4 h before measurements were recorded, and chamber measurements were conducted for a minimum of 6 h.

TDL absorption spectroscopy measurements

The TDL sampled both the inlet and the outlet of the soil chamber at a frequency of one measurement cycle every 2 min. Each cycle consisted of measurements of two calibration standards followed by measurements of samples from the chamber inlet and outlet. A multiport manifold was used to direct flow from each inlet into the sample path of the TDL for a total of 30 s with the last 15 s averaged for each measurement. Determinations of mole fractions for $^{12}\text{C}^{16}\text{O}_2$, $^{13}\text{C}^{16}\text{O}_2$, and $^{12}\text{C}^{18}\text{O}^{16}\text{O}$ were corrected during post-processing by applying a linear correction to each measurement cycle, derived from the difference between the measured and actual values of the calibration standards.²¹ Using three or more points for calibration is critical over large $[\text{CO}_2]$ ranges;⁴¹ however, tests of the two-point calibration carried out concurrently with this study exhibited high accuracy.⁴² We repeated the test of Bickford *et al.*⁴² predicting the $\delta^{13}\text{C}$ and $\delta^{18}\text{O}$ of a $550 \mu\text{mol mol}^{-1}$ gold standard cylinder using $150 \mu\text{mol mol}^{-1}$ and $350 \mu\text{mol mol}^{-1}$ gold standard calibrations. Differentials between predicted and observed values were -0.03‰ for $\delta^{13}\text{C}$, 0.46‰ for $\delta^{18}\text{O}$, and $0.20 \mu\text{mol mol}^{-1}$ for $[\text{CO}_2]$. Numerous working calibration cylinders were used throughout the experiment, all of which had $[\text{CO}_2]$, $\delta^{13}\text{C}$ and $\delta^{18}\text{O}$ values similar to

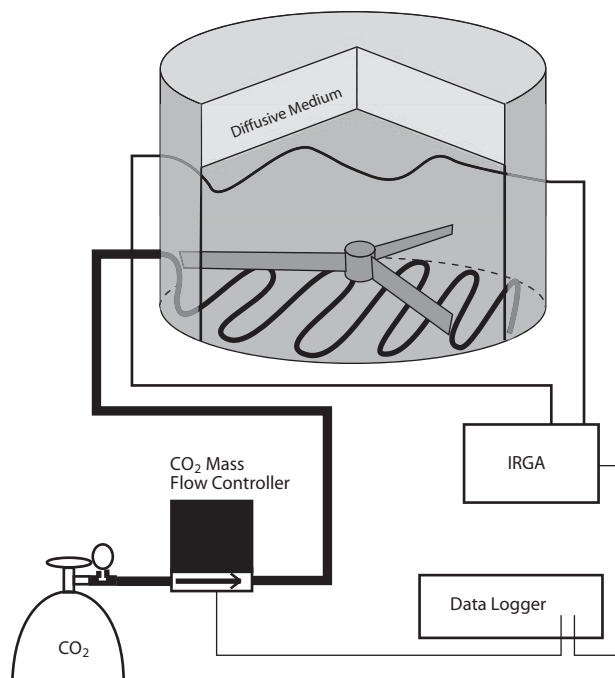


Figure 2. Schematic of the constant-flux test column used in this study. The system produces known and stable surface CO_2 effluxes with known values of $\delta^{13}\text{C}$ and $\delta^{18}\text{O}$ and is used to test the accuracy of a soil chamber. By constantly monitoring and adjusting $[\text{CO}_2]$ below the diffusive medium, constant diffusion gradients can be maintained and produce constant surface fluxes. By measuring $\delta^{13}\text{C}$ and $\delta^{18}\text{O}$, the isotopic composition of the surface efflux can be determined. See Experimental section for further details.

those of our WMO (World Meteorological Organization) certified standards from which they were propagated monthly. The gold standards values were: high standard: $[\text{CO}_2] = 548.16 \mu\text{mol mol}^{-1}$, $\delta^{13}\text{C} = -16.42\text{‰}$, $\delta^{18}\text{O} = 20.56\text{‰}$; low standard: $[\text{CO}_2] = 344.88 \mu\text{mol mol}^{-1}$, $\delta^{13}\text{C} = -8.16\text{‰}$, $\delta^{18}\text{O} = 28.84\text{‰}$. The corresponding high $[\text{C}^{16}\text{O}_2]$ equaled $539.57 \mu\text{mol mol}^{-1}$ (high standard) and $339.43 \mu\text{mol mol}^{-1}$ (low standard), $[\text{C}^{13}\text{C}^{16}\text{O}_2]$ equaled $5.9332 \mu\text{mol mol}^{-1}$ (high standard) and $3.7638 \mu\text{mol mol}^{-1}$ (low standard), and $[\text{C}^{12}\text{C}^{18}\text{O}^{16}\text{O}]$ equaled $2.2084 \mu\text{mol mol}^{-1}$ (high standard) and $1.4005 \mu\text{mol mol}^{-1}$ (low standard). These WMO standards were used to calibrate all other cylinders used in this study (described below). Corrected isotopologue values were converted and expressed relative to the known standards VPDB for $\delta^{13}\text{C}$ and VSMOW for $\delta^{18}\text{O}$. For the $[\text{CO}_2]$ values used in Eqns. (1) and (2), measured isotopologue values were summed and a fraction for all other non-measured isotopologues was added.⁴³

Soil watering experiment

The field tests were conducted at Mesita del Buey, a piñon-juniper woodland located outside our TDL facility at Los Alamos National Laboratory in northern New Mexico, USA. The site is at an elevation of 2140 m; has annual precipitation of ~ 400 mm, mainly in the form of winter snowfall and late-summer precipitation; mean ambient air temperature of $\sim 9^\circ\text{C}$, ranging from -2°C in January to 21°C in June; and soil

depths varying between 33 and 125 cm. The soil is a Hackroy sandy loam developed from Bandelier Tuff parent material.⁴⁴ The woodland is dominated by *Juniperus monosperma* with a small fraction of *Pinus edulis*. Further details regarding Mesita del Buey can be found in Breshears *et al.*⁴⁵

The soil chamber was configured in the same manner as for the test column. One day prior to measurements, collars were placed in the soil to allow the CO_2 efflux to stabilize from disturbance after collar placement.⁷ After adjusting the chamber flow rate and equalizing the chamber pressure with the atmosphere, the chamber was placed on the collar and sealed with water. Data for the chamber inlet and outlet $[\text{CO}_2]$, $\delta^{13}\text{C}$ and $\delta^{18}\text{O}$ were collected every 2 min with the TDL, and chamber outlet $[\text{CO}_2]$ and water vapor were collected at 1 Hz with the IRGA and logged with the data logger. The $[\text{CO}_2]$ in the chamber headspace was allowed to stabilize and data was collected for at least 30 min prior to water addition. After the initial stabilization and measurement period, a simulated 50 mm rain event was added via the watering manifold to evenly wet the soil and without removing the soil chamber. Water addition was carried out over approximately a 4 min period to prevent any water from standing on the soil surface. Data was collected continuously before, during and after the watering event.

We collected leaf material from five individuals of the most dominant plants at the field site (*Juniperus monosperma*, *Bouteloua gracilis*, *Gutierrezia sarothrae*, *Lolium perenne*, *Erigeron divergens*, *Sisymbrium altissimum*) for analyses of $\delta^{13}\text{C}$ and soil water for analyses of $\delta^{18}\text{O}$ in order to compare with observed $\delta^{13}\text{C}_\text{R}$ and $\delta^{18}\text{O}_\text{R}$ values. Foliage was collected from sun-exposed aspects, dried to constant mass, and ground with a mortar and pestle. Soil water was collected within 15 min after removal of the soil chamber from directly beneath the chamber and from an adjacent location with non-watered soil for analyses of the impact of watering on soil water content and soil water $\delta^{18}\text{O}$. Soil was collected from the 0–10 cm depth as well as in depth profiles from the top 15 cm of soil (2 cm, 5 cm, 8 cm, 11 cm, and 15 cm). The soil water content was measured gravimetrically along this profile. Samples for $\delta^{18}\text{O}$ analyses were immediately stored in glass vials wrapped with wax film and kept frozen until analyses. Water was extracted by cryogenic vacuum distillation and $\delta^{18}\text{O}$ was analyzed by isotope ratio mass spectrometry. Samples were analyzed on a Eurovector elemental analyzer (Milan, Italy) coupled to a Micromass Isoprime isotope ratio mass spectrometer (GV Instruments, Manchester, UK) operated in continuous flow mode at Los Alamos National Laboratory Stable Isotope Lab (NM, USA). Nitrous oxide and CO_2 were separated by gas chromatography and corrections for the contribution of $^{12}\text{C}^{17}\text{O}^{16}\text{C}$ to mass 33 were made for all runs. The overall precision for $\delta^{13}\text{C}$ was 0.09‰ ($n = 8$) and for $\delta^{18}\text{O}$ it was 0.31‰ ($n = 24$). The $\delta^{18}\text{O}$ value of CO_2 in equilibrium with soil water was calculated using the soil water $\delta^{18}\text{O}$ value from the top 15 cm and the soil temperature measured at 5 cm, along with the equations of Brenninkmeijer *et al.*³⁶

$$\varepsilon_w = \frac{17604}{T_1} - 17.93 \quad (3)$$

where ε_w (‰) is the temperature-dependent ^{18}O fractionation between CO_2 and water at equilibrium.

RESULTS

Rates of CO₂ efflux generated in the test column and quantified via the TDL system were compared with the more widely used IRGA measurements, and the two methods yielded similar results (Fig. 3, linear regression $R^2=0.99$, $p<0.0001$). The TDL-chamber measurements of efflux rates from the column were in good agreement with the column efflux rates, which we considered the benchmark for our efflux rate tests (Fig. 4). For combined chamber flow-through rates, the chamber measurements of column CO₂ effluxes were not significantly different from known values ($p=0.54$). There was a linear relationship for all data (slope=0.95, $R^2=0.94$) and for the 300 and 500 mL min⁻¹ flow rates separately (slope=0.68, $R^2=0.93$ and slope=0.94 and $R^2=0.95$, respectively). Both showed no significant differences in measured efflux from known rates ($p=0.35$ and $p=0.87$ for the 300 and 500 mL min⁻¹ flow rates, respectively).

For all flow rates and efflux rates with the test column, the $\delta^{13}\text{C}_\text{R}$ and $\delta^{18}\text{O}_\text{R}$ measurements from the chamber were not significantly different from the expected values of $-39.0 \pm 0.3\text{‰}$ and $9.7 \pm 0.3\text{‰}$ ($\delta^{13}\text{C}_\text{R}$ and $\delta^{18}\text{O}_\text{R}$, respectively) with observed $\delta^{13}\text{C}_\text{R}$ of $-38.9 \pm 0.6\text{‰}$ ($p=0.66$) and $\delta^{18}\text{O}_\text{R}$ of $9.6 \pm 1.1\text{‰}$ ($p=0.81$, Fig. 5). Likewise, individual comparisons by flow rate did not show any significant differences between the expected and measured values, with observations at 300 mL min⁻¹ of $-39.3 \pm 0.6\text{‰}$ ($\delta^{13}\text{C}_\text{R}$, $p=0.40$) and $9.0 \pm 1.0\text{‰}$ ($\delta^{18}\text{O}_\text{R}$, $p=0.21$) and at 500 mL min⁻¹ of $-38.7 \pm 0.5\text{‰}$ ($\delta^{13}\text{C}_\text{R}$, $p=0.13$) and $10.1 \pm 0.9\text{‰}$ ($\delta^{18}\text{O}_\text{R}$, $p=0.34$).

Field measurements showed an average efflux rate of $0.3 \pm 0.05 \mu\text{mol CO}_2 \text{ m}^{-2} \text{ s}^{-1}$ for dry soils prior to watering

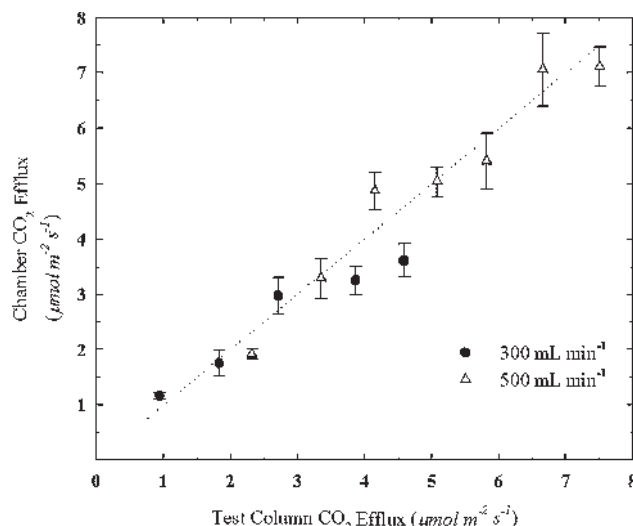


Figure 4. Comparison of TDL-chamber measurements of CO₂ efflux with known CO₂ efflux from the test column. Flow-through rates of 300 mL min⁻¹ (closed symbols) and 500 mL min⁻¹ (open symbols) were tested. A 1:1 line (dashed) is shown for comparison.

(Fig. 6). The isotopic values of dry soil CO₂ efflux had values of $\delta^{13}\text{C}_\text{R} = -20.6 \pm 3.0\text{‰}$ and $\delta^{18}\text{O}_\text{R} = 80.3 \pm 7.7\text{‰}$. Addition of a simulated 50 mm rain event to the soil caused a 24-fold increase in efflux to $7.2 \pm 0.5 \mu\text{mol m}^{-2} \text{ s}^{-1}$. The water addition changed the $\delta^{13}\text{C}_\text{R}$ by -5.0‰ to $-25.6 \pm 0.7\text{‰}$ and the $\delta^{18}\text{O}_\text{R}$ by -55.0‰ to $25.3 \pm 1.2\text{‰}$. The efflux, $\delta^{13}\text{C}$ and $\delta^{18}\text{O}$ responses were detectable within the first measurement cycle after initiation of the water addition (i.e. 2 min). The CO₂ efflux reached maximum values within 20 min, and the $\delta^{13}\text{C}$ and $\delta^{18}\text{O}$ both reached maximum responses within 10 min. Notably, the pre-watering standard deviations were large due to the relatively small [CO₂] difference between inlet and outlet associated with low rates of soil respiration. For example, if the chamber $c_0 = 420 \mu\text{mol mol}^{-1}$ and

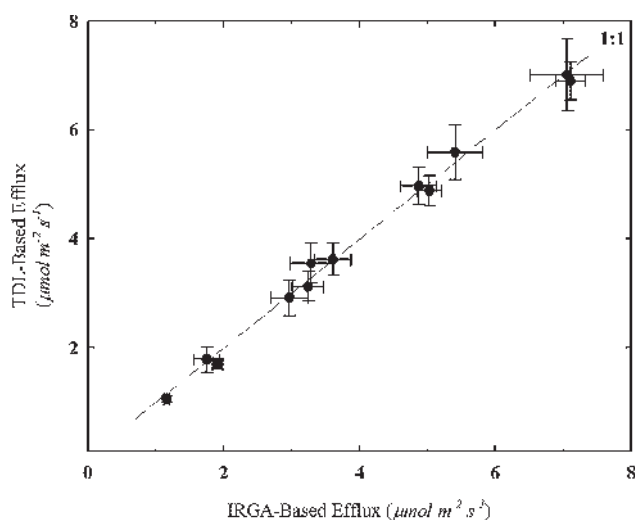


Figure 3. Comparison of TDL-derived CO₂ efflux measurement and independent IRGA measurements (LI-840). In both cases the chamber CO₂ efflux rate ($\mu\text{mol m}^{-2} \text{ s}^{-1}$) was calculated based on the difference in CO₂ concentration between the air entering and the air exiting the chamber (Eqn. (1)). A 1:1 line (dashed) is shown for comparison. The least means squared regression equation is: $y = 0.99x - 0.02$, $R^2 = 0.99$.

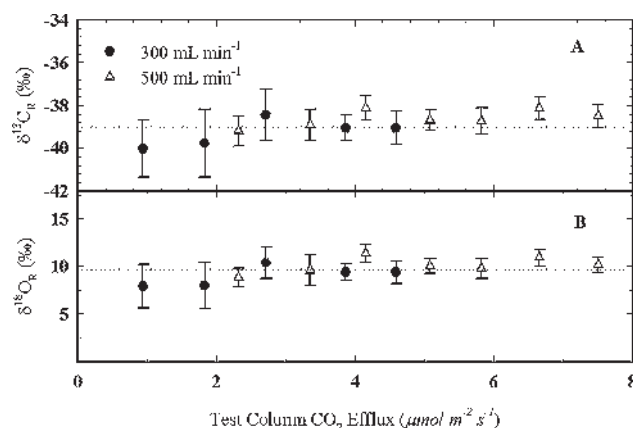


Figure 5. TDL-chamber measurements of (A) $\delta^{13}\text{C}_\text{R}$ and (B) $\delta^{18}\text{O}_\text{R}$ across a range of CO₂ efflux rates using the test-column system. Dashed lines represent known isotopic values. Flow rates of 300 mL min⁻¹ (closed symbols) and 500 mL min⁻¹ (open symbols) are shown.

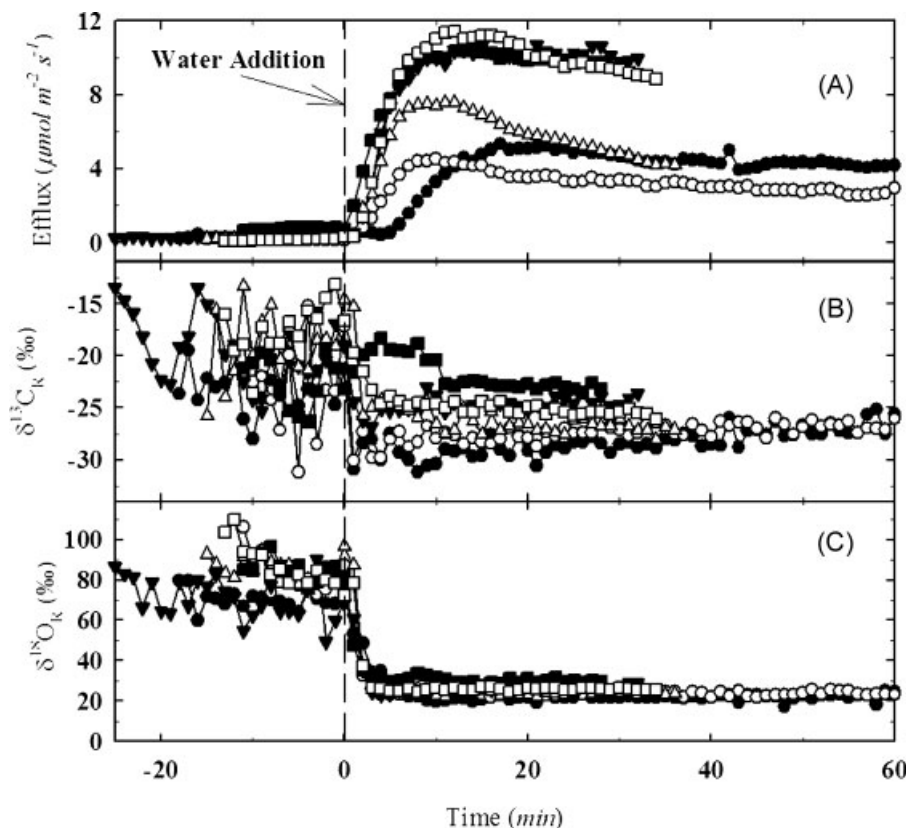


Figure 6. Field measurements of (A) soil CO_2 efflux rates, (B) $\delta^{13}\text{C}_\text{R}$ and (C) $\delta^{18}\text{O}_\text{R}$ from six locations in a piñon-juniper woodland. A 50 mm rain event was simulated through application of 792 mL of water through a port within the chamber (represented as time 0).

$c_i = 400 \mu\text{mol mol}^{-1}$, a measurement error of 0.05‰ for both δ_o and δ_i changes the δ_R value by 2‰ . In contrast, if the CO_2 differential is raised to $50 \mu\text{mol mol}^{-1}$ ($c_\text{o} = 450$ and $c_i = 400 \mu\text{mol mol}^{-1}$), the same error changes the δ_R by 0.8‰ .

The addition of water increased the gravimetric water content of the dry soil (0–10 cm depth) by 5-fold, from an average of 2.8% to 14.2% and changed the $\delta^{18}\text{O}$ of soil water from $2.8 \pm 1.7\text{‰}$ to $-8.3 \pm 1.8\text{‰}$ (Table 1, the added water $\delta^{18}\text{O} = -10.85\text{‰}$). Calculating the $\delta^{18}\text{O}$ of CO_2 in equilibrium with the observed $\delta^{18}\text{O}$ of soil water using Eqn. (3) and the observed soil temperature at 10 cm depth gives pre- and post-watering values of 45.6‰ and 34.0‰ . The leaf $\delta^{13}\text{C}$ of nearby plants averaged $-26.48 \pm 1.8\text{‰}$. Species averages were: *Bouteloua gracilis* $-16.0 \pm 0.10\text{‰}$, *Juniperus monosperma* $-24.3 \pm 0.33\text{‰}$, *Gutierrezia sarothrae* $-29.0 \pm 0.43\text{‰}$, *Lolium*

perenne $-29.4 \pm 0.21\text{‰}$, *Erigeron divergens* $-29.95 \pm 0.61\text{‰}$, and *Sisymbrium altissimum* $-27.95 \pm 0.25\text{‰}$.

DISCUSSION

The soil chamber used in this study provided measurements of soil CO_2 efflux, $\delta^{13}\text{C}_\text{R}$, and $\delta^{18}\text{O}_\text{R}$ that were both accurate (Figs. 3–5) and rapid (Fig. 6). Since *TDL* absorbance spectroscopy is a relatively new technology for application to chamber-based measurements, we verified the accuracy of the CO_2 efflux via simultaneous measurements with a previously tested *IRGA*. There was a linear relationship between the *TDL*-based and *IRGA*-based measurements with the values falling along the 1:1 line, and both techniques had comparable degrees of variation (Fig. 3). With verification of

Table 1. Soil water content and CO_2 - $\delta^{18}\text{O}$ values in the field experiment before and after the addition of water. Soil CO_2 - $\delta^{18}\text{O}$ is calculated from measurements of soil-water $\delta^{18}\text{O}$, soil temperature and Eqn. (3). See Experimental section for more details

Depth (cm)	Soil water content (%)		Soil CO_2 - $\delta^{18}\text{O}$ (‰)	
	Before watering	After watering	Before watering	After watering
2	2.35	16.58	41.14	23.16
5	2.53	14.73	46.53	24.05
8	2.91	13.13	45.41	24.99
11	4.08	13.13	45.30	25.61
15	4.99	11.62	43.31	27.65

this component completed, we then focused on the challenging measurement aspects of chamber-based isotopic flux measurements. The system performed well overall, although potential sources of error were identified that can be minimized in future applications. It is worth noting that the use of glass beads for the diffusive medium in the accuracy tests (Figs. 2, 3–5) resulted in a 'soil' medium that was more permeable than nearly all vegetated soils on earth; thus our tests were highly conservative for chamber-induced anomalies.⁴⁶ The high permeability offered very little resistance to mass flow of CO₂ into or out of the beads, so small pressure artifacts from the chamber (the most likely errors) caused immediately detectable changes in CO₂ efflux.

The *TDL*-chamber measurements showed relatively good agreement with the column effluxes over a wide range of efflux rates at two chamber flow rates (Fig. 4). For the chamber flow rate of 300 mL min⁻¹, the data adhered to the 1:1 line very well at lower efflux rates but underestimated fluxes at the two highest rates. This may have resulted from the proportional increase in chamber headspace [CO₂] with rising efflux rates, which reduced the CO₂ diffusion gradient into the chamber and subsequently impacted the efflux. A solution to this problem is to use higher system flow rates (i.e. 500 mL min⁻¹) to measure high CO₂ efflux rates. High test column (or soil-respired) efflux rates also increased the amount of time needed for the [CO₂] in the headspace to reach steady state. Although the pressure of the chamber was equalized to that of the atmosphere prior to placing the chamber on the collar, long periods for measurement stabilization may have allowed more time for pressure anomalies to develop that could cause errors in chamber measurements.⁴⁶

Measurements of $\delta^{13}\text{C}_\text{R}$ and $\delta^{18}\text{O}_\text{R}$ showed that the *TDL*-chamber method is statistically valid for determining the isotopic composition of soil-respired CO₂ (Fig. 5) at all tested efflux rates. However, δ_R was slightly depleted at low efflux rates and enriched at high efflux rates relative to known values. Errors at high efflux may occur due to reduced diffusion gradients (as listed above) or perhaps, due to insufficient mixing, creating a surface boundary layer that biases observations towards inlet δ_R values, especially at higher flow-through rates. The slight depletion and relative large uncertainty in $\delta^{13}\text{C}_\text{R}$ and $\delta^{18}\text{O}_\text{R}$ observed for the two measurements at the lowest efflux rates (Fig. 5) could be caused by changes in the test column CO₂ isotopic composition over the course of their measurements because of there being an isotopic non-steady state in the test column. This could occur because, immediately before the experiment, CO₂ was scrubbed from the column and replaced with -41.3‰ ($\delta^{13}\text{C}$) CO₂ from a cylinder. The lowest efflux rate tests were conducted within 24 h of scrubbing the column, during which time atmospheric air from the laboratory may have diffused into the column, enriching the column $\delta^{13}\text{C}$ above the cylinder isotopic values (i.e. -41.3‰ for $\delta^{13}\text{C}$). This invasion of isotopically heavier ambient CO₂ may have shifted the effective 'source' CO₂ to the observed value of -39.0‰ (after correction for diffusive fractionation)³⁵ during the course of the two lowest efflux rate tests. Later measurements were conducted at least 3 days after scrubbing CO₂ from the column and allowed sufficient time for isotopic

steady state within the test column to be achieved, resulting in less variability (Fig. 5). To capture any changes to the source air beneath the porous medium, future tests should continuously measure $\delta^{13}\text{C}$, $\delta^{18}\text{O}$, and [CO₂] in the column volume.

Comparison of the *TDL*-chamber measurements of δ_R in our study with results from previous soil respiration systems that utilized mass spectrometry is hampered by lack of empirical tests conducted in the past. Most previous systems only provided estimates of mass spectrometer precision from repeated measurements on the mass spectrometer, rather than from the entire system. The *TDL* precision tested through repeated measurements of cylinders in our study ranged from 0.10‰ to 0.17‰ for $\delta^{13}\text{C}$ and from 0.17‰ to 0.25‰ for $\delta^{18}\text{O}$. The $\delta^{13}\text{C}$ precision can be improved if $\delta^{18}\text{O}$ measurements are forgone since there are more strongly absorbing spectral lines used by the *TDL* system when $\delta^{13}\text{C}$ is measured exclusively. Mass spectrometry measurements conducted in our lab, using the same working cylinders as used in the *TDL* study, had standard deviations of 0.05‰ for $\delta^{13}\text{C}$ and 0.08‰ for $\delta^{18}\text{O}$. This is typical for gas source isotope ratio mass spectrometers, e.g. 0.01‰ to 0.15‰ for $\delta^{13}\text{C}$ and up to 0.20‰ for $\delta^{18}\text{O}$.^{16,21,47} Prior reports of *TDL* precision from repeated sampling of known cylinders gave ranges from 0.03‰ to 4.0‰ for $\delta^{13}\text{C}$,⁴⁸ and 0.20‰ for $\delta^{18}\text{O}$.⁴³ The precision of the entire system is lower, however, due to the combined errors associated with sample collection.^{41,43} For this study, we report the system precision of the entire system to be 0.6‰ and 1.1‰ for $\delta^{13}\text{C}_\text{R}$ and $\delta^{18}\text{O}_\text{R}$, respectively (Fig. 5), which is comparable with our previous whole-system *TDL* measurements on foliage (0.5 to 1.99‰ for $\delta^{13}\text{C}_\text{R}$ and 1.1 to 5.1‰ for $\delta^{18}\text{O}_\text{R}$).^{43,49} We are aware of no other empirical tests of chamber-based measurements of $\delta^{13}\text{C}_\text{R}$ and $\delta^{18}\text{O}_\text{R}$; however, numerical model analyses suggest that most systems have positive biases of 1 to 3‰ for $\delta^{13}\text{C}_\text{R}$.²⁶

Water addition experiment

High temporal resolution sampling of soil CO₂ efflux, $\delta^{13}\text{C}_\text{R}$ and $\delta^{18}\text{O}_\text{R}$ isotope values from the chamber captured large shifts in response to water addition to a dry field soil (Fig. 6). Changes were detectable within 2 min of watering for both CO₂ efflux and δ_R , and the maximum response was achieved within 20 and 10 min, respectively. Prior to water addition, the soil efflux was less than 1 $\mu\text{mol m}^{-2} \text{s}^{-1}$. This was consistent with field measurements conducted at a nearby site using a LI-COR 6400-09 soil chamber (LI-COR Biosciences) and is typical for dry conditions during the late spring drought in this region (data not shown). The δ_R measurements had high standard deviations during the pre-watering period because the differential between chamber inlet and outlet [CO₂] was small (<30 $\mu\text{mol mol}^{-1}$), which leads to poor precision. This is due to the large impact on the δ_R values resulting from errors in δ_o and δ_i measurements when there is a small difference in c_o and c_i in Eqn. (2) (see Results section for example calculations).

The addition of a 50 mm watering event caused a large shift in both the efflux rate and the isotopic composition. On average there was a 6.9 $\mu\text{mol m}^{-2} \text{s}^{-1}$ increase in CO₂ efflux; an increase of nearly 24-fold. The initial increase in CO₂ efflux could be attributed to the displacement of CO₂ in the

soil from the 792 mL of water that were added; however, we saw only one soil collar that exhibited a pulse of CO_2 before returning to a stable, elevated flux (Fig. 6(A)). Based on the displacement of 792 mL of soil gas with a conservative, maximum estimated $[\text{CO}_2]$ of $2000 \mu\text{mol mol}^{-1}$,^{50,51} the increase in soil CO_2 efflux cannot be explained solely by displacement (Fig. 7). All soil collar measurements showed a sustained increase in CO_2 efflux until the measurements were terminated, at least 60 min after water addition. Although further work is necessary to attribute mechanistic causes, it seems likely that this response was dominated by increased microbial activity.^{15,24}

The addition of water to the chamber also produced an average shift of -5.0‰ for $\delta^{13}\text{C}_\text{R}$, from -20.6‰ to -25.6‰ (Fig. 6(B)). We do not know what caused the shift in $\delta^{13}\text{C}_\text{R}$ but we speculate that is due to an increase in heterotrophic activity. Since the soil at this site is very low in carbonates, we do not expect any contribution from carbonates to affect the efflux $\delta^{13}\text{C}$ values. We can also exclude changes in photosynthetic discrimination of nearby vegetation because the water was applied over a small area and the responses were seen within 2 min, far too fast for a photosynthetic signal to travel to the soil. The shift in $\delta^{13}\text{C}_\text{R}$ is consistent with a shift from live root respiration of *Juniperus* and *Bouteloua* plants (average leaf $\delta^{13}\text{C}$ of -20.0‰) to heterotrophic consumption of other substrates, such as dead organic matter from *Gutierrezia*, *Erigeron*, and *Lolium* (average leaf $\delta^{13}\text{C}$ of -29.5‰). This is consistent with previous observations of pulse rain events initiating respiratory responses from heterotrophic organisms in soils that were inactive under dry conditions, prompting a shift in the substrates used for decomposition.^{15,24,52,53} A mutually inclusive hypothesis is that wetting shifted the depth of dominant respiration upwards towards the surface because soil carbon

$\delta^{13}\text{C}$ is typically more depleted at upper depths and enriched at deeper depths.⁵⁴

The $\delta^{18}\text{O}_\text{R}$ value dropped by -55‰ after water was added within the soil collar, from 80.3‰ to 25.3‰ . That this large shift occurred is expected because the theoretical $\delta^{18}\text{O}$ of CO_2 produced from the tap water is 31.4‰ , and the amount of water added was equivalent to the largest 1% of rain storms recorded at this site over the last 15 years. The $\delta^{18}\text{O}_\text{R}$ observed pre- and post-watering was not predicted based on soil water $\delta^{18}\text{O}$, however, regardless of the assumed setting point depth and degree of kinetic fractionation due to diffusion¹⁸ (Table 1). The pre-watering $\delta^{18}\text{O}_\text{R}$ value was under-predicted by 34.5‰ (80‰ observed vs. 45.6‰ predicted). Caution must be observed in interpreting this result because water was added to a small area surrounded by dry soil; the lateral diffusion impacts may have influenced our observations.²⁶ Using the most enriched $\delta^{18}\text{O}$ soil water measurements reduces the difference by only 1‰ . We assume that our $\delta^{18}\text{O}_\text{R}$ measurements are accurate based on our tests (Fig. 5) and because nightly, ecosystem-scale Keeling plots generated from data collected with the TDL at this site gave intercepts between 54‰ and 68‰ , closer to the soil chamber data. In a similar study on relatively dry soils in which the observed $\delta^{18}\text{O}_\text{R}$ was more enriched than predicted, Wingate *et al.*⁵⁵ concluded that model observation discrepancy was explained by unquantified, highly enriched water near the surface and by higher than expected invasion, facilitated by the hydration mechanism of the enzyme carbonic anhydrase. Although more measurements are required to test these mechanisms,⁵⁵ we agree with this interpretation. Our shallowest soil water $\delta^{18}\text{O}$ data was collected at 2 cm, and we may thus have missed enrichment of soil water pools near the soil surface. Likewise, the hypothesis that our soils were experiencing a high degree of invasion by atmospheric air

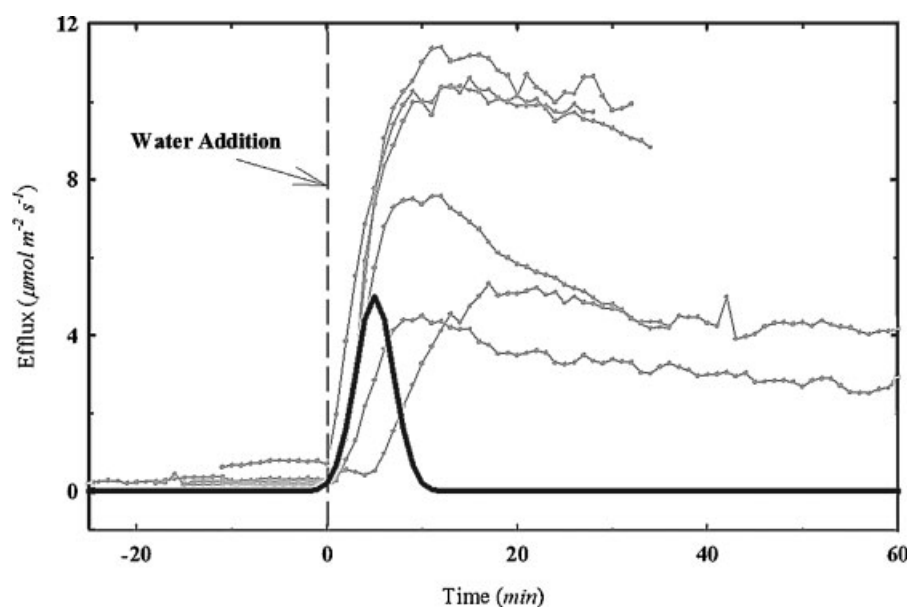


Figure 7. The potential contribution of displacement of soil CO_2 to the increased respiration rates observed in Fig. 6. The bold line shows the contribution to CO_2 efflux that could occur from displacing soil gas during the water addition. Gray lines show chamber CO_2 efflux rates for comparison. Displacement equivalent to 792 mL of soil gas (from water volume) with $2000 \mu\text{mol mol}^{-1}$ $[\text{CO}_2]$ is equivalent to $25 \mu\text{mol}$ of CO_2 . This is represented as the area under the bold curve.

with relatively positive $\delta^{18}\text{O}$ values is likely due to our extremely dry conditions that result in highly permeable soils. This conclusion is supported by the much closer model-observation agreement post-watering, when invasion impacts should be lessened by the filling of pore space with water. We note that the pre-watering soil water content at 2 cm depth of 2.8% should result in higher atmospheric invasive influence than found by Wingate *et al.*,⁵⁵ who reported minimum soil water contents of $\sim 8.0\%$.

For post-watering observations, the difference between predicted and observed $\delta^{18}\text{O}_\text{R}$ is much smaller than for pre-watering measurements, although an offset remained. The observed $\delta^{18}\text{O}_\text{R}$ of 25.0‰ is lighter than predicted (34.0‰) by approximately the full theoretical value of the kinetic fractionation during diffusion of 8.8‰.³⁴ One interpretation of this result is that the time to reach isotopic equilibrium may be longer than the 120 min that we observed (e.g. 3–6 h).⁵⁶ An important point to note is that the dry-soil $\delta^{18}\text{O}_\text{R}$ values are so enriched that, despite the low rates of respiration, the iso-flux could be very large and thus have a significant impact on regional or global carbon cycles using isotopes for parameterization.⁵⁷ Likewise, the dramatic pulse response of $\delta^{18}\text{O}_\text{R}$ and $\delta^{13}\text{C}_\text{R}$ could impart large, detectable signals on the atmospheric $\delta^{13}\text{C}$ and $\delta^{18}\text{O}$.

One final measurement challenge should be noted for field applications of the TDL-chamber system. Since the TDL was on a 30 s measurement cycle, there is a 30 s lag between measurements of the chamber inlet and outlet gases. This could be problematic if there were significant and rapid changes in inlet $[\text{CO}_2]$ such as caused by wind-induced pressure-pumping.⁵⁸ The use of a compressed gas cylinder minimizes this problem by maintaining a constant isotope and concentration source. In our study, measurements of the inlet $[\text{CO}_2]$ and isotopic composition by TDL showed very little variance (standard deviation = $0.18 \mu\text{mol mol}^{-1}$) and the fluxes measured by both TDL and IRGA corresponded closely (Fig. 3).

CONCLUSIONS

Our data show that the soil chamber-TDL system was capable of measuring soil efflux and isotopic composition effectively and with high frequency. When the soil chamber was used with a test column where the efflux rate and isotopic composition were tightly controlled, the chamber measurements closely matched the column efflux rate and had average differences of -0.08% for $\delta^{13}\text{C}_\text{R}$ and -0.08% for $\delta^{18}\text{O}_\text{R}$. We found no statistical difference between measured and known values for either fluxes or δ_R . Our results confirm prior observations that careful regulation of pressure artifacts and consideration of flow rates relative to CO_2 efflux rates is warranted. High-frequency measurements captured rapid changes in soil CO_2 efflux and δ_R after pulse watering events (Fig. 6), allowing detection of events that might otherwise be missed. Sampling on a lower frequency time scale of hours or days would probably not capture the fast responses seen here with sufficient resolution to determine the time after watering in which a response occurs and the magnitude of the changes at their maxima.

Acknowledgements

We thank Will Pockman for help in determining the course of this research and for helpful comments on the draft manuscript. Thanks to Clif Meyer, Dave Bowling, Dan Breecker and Bill Riley for helpful input and technical assistance. Thanks to Steve Sargent for help with laser spectroscopy. Thank to Dan Breecker and two other anonymous reviewers for helpful comments. This work was funded by a Laboratory Directed Research and Development grant to NM, and to NM and DH grants from the Institute for Geophysical and Planetary Physics and the National Science Foundation (IOS-0719118).

REFERENCES

- Bender MM. *Phytochemistry* 1971; **10**: 1239.
- Miller JB, Tans PP, White JWC, Conway TJ, Vaughn BW. *Tellus. Series B, Chem. Phys. Meteorol.* 2003; **55B**: 197.
- Yakir D, Wang XF. *Nature* 1996; **380**: 515.
- Ciais P, Tans PP, White JWC, Trolier M, Francey RJ, Berry JA, Randall DR, Sellers PJ, Collatz JG, Schimel DS. *J. Geophys. Res. – Atmospheres* 1995; **100**: 5051.
- Raich JW, Schlesinger WH. *Tellus Series B, Chem. Phys. Meteorol.* 1992; **44**: 81.
- Randerson JT, Chapin FS, Harden JW, Neff JC, Harmon ME. *Ecol. Appl.* 2002; **12**: 937.
- Law BE, Baldocchi DD, Anthoni PM. *Agric. Forest Meteorol.* 1999; **94**: 171.
- Bowling D, McDowell N, Bond B, Law B, Ehleringer J. *Oecologia* 2002; **131**: 113.
- Farquhar GD, Lloyd J, Taylor JA, Flanagan LB, Syvertsen JP, Hubick KT, Wong SC, Ehleringer JR. *Nature* 1993; **363**: 439.
- Riley WJ. *Geochim. Cosmochim. Acta* 2005; **69**: 1939.
- Fung I, Field CB, Berry JA, Thompson MV, Randerson JT, Malmstrom CM, Vitousek PM, Collatz GJ, Sellers PJ, Randall DA, Denning AS, Badeck F, John J. *Global Biogeochem. Cycles* 1997; **11**: 507.
- Randerson JT, Still CJ, Balle JJ, Fung IY, Doney SC, Tans PP, Conway TJ, White JWC, Vaughn B, Suits N, Denning AS. *Global Biogeochem. Cycles* 2002; **16**: 1028.
- Cerling TE. *Earth Planet. Sci. Lett.* 1984; **71**: 229.
- Ehleringer JR, Buchmann N, Flanagan LB. *Ecol. Appl.* 2000; **10**: 412.
- Cable JM, Huxman TE. *Oecologia* 2004; **141**: 317.
- McDowell NG, Bowling DR, Bond BJ, Irvine J, Law BE, Anthoni P, Ehleringer JR. *Global Biogeochem. Cycles* 2004; **18**: GB1013.
- Ekblad A, Hogberg P. *Plant Soil* 2000; **219**: 197.
- Miller JB, Yakir D, White JWC, Tans PP. *Global Biogeochem. Cycles* 1999; **13**: 761.
- Marron N, Plain C, Longdoz B, Epron D. *Plant Soil* 2009; **318**: 137.
- Bahn M, Schmitt M, Siegwolf R, Richter A, Brueggemann N. *New Phytologist* 2009; **182**: 451.
- Bowling D, Sargent S, Tanner B, Ehleringer J. *Agric. Forest Meteorol.* 2003; **118**: 1.
- Griffis TJ, Lee X, Baker JM, Sargent SD, King JY. *Agric. Forest Meteorol.* 2005; **135**: 44.
- McDowell NG, Baldocchi DD, Barbour MM, Bickford CP, Cuntz M, Hanson DT, Knohl A, Powers HH, Rahn T, Riley WJ, Walcroft A. *EOS* 2008; **89**: 94.
- Jarvis P, Rey A, Petsikos C, Wingate L, Rayment M, Pereira J, Banza J, David J, Miglietta F, Borghetti M, Manca G, Valentini R. *Tree Physiol.* 2007; **27**: 929.
- Kayler ZE, Sulzman EW, Marshall JD, Mix A, Rugh WD, Bond BJ. *Rapid Commun. Mass Spectrom.* 2008; **22**: 2533.
- Nickerson N, Risk D. *Rapid Commun. Mass Spectrom.* 2009; **23**: 2802.
- Nickerson N, Risk D. *Geophys. Res. Lett.* 2009; **36**: L08401.
- Davidson EA, Savage K, Verchot LV, Navarro R. *Agric. Forest Meteorol.* 2002; **113**: 21.
- Widen B, Lindroth A. *Soil Sci. Soc. Am. J.* 2003; **67**: 327.
- Fang C, Moncrieff JB. *Funct. Ecol.* 1996; **10**: 297.

31. Norman JM, Kucharik CJ, Gower ST, Baldocchi DD, Crill PM, Rayment M, Savage K, Striegl RG. *J. Geophys. Res.* 1997; **102**: 28771.
32. Rayment MB, Jarvis PG. *J. Geophys. Res.* 1997; **102**: 28779.
33. Evans JR, Sharkey TD, Berry JA, Farquhar GD. *Aust. J. Plant Physiol.* 1986; **13**: 281.
34. Cerling TE, Solomon DK, Quade J, Bowman JR. *Geochim. Cosmochim. Acta* 1991; **55**: 3403.
35. Amundson R, Stern L, Baisden T, Wang Y. *Geoderma* 1998; **82**: 83.
36. Brenninkmeijer CAM, Kraft P, Mook WG. *Isot. Geosci.* 1983; **1**: 181.
37. Mook WG, Bommerson JC, Staverman WH. *Earth Planet. Sci. Lett.* 1974; **22**: 169.
38. Kapiluto Y, Yakir D, Tans P, Berkowitz B. *Geochim. Cosmochim. Acta* 2007; **71**: 2657.
39. Ball TJ. Calculations related to gas exchange. In *Stomatal Function Meeting: Honolulu, USA, April 1983*, Zeiger E, Farquhar GD, Cowan IR (eds). Stanford University Press: Stanford, USA. 1987; 445.
40. Martin JG, Bolstad PV, Norman JM. *Soil Sci. Soc. Am. J.* 2004; **68**: 514.
41. Bowling DR, Burns SP, Conway TJ, Monson RK, White JWC. *Global Biogeochem. Cycles* 2005; **19**: GB3023.
42. Bickford CP, McDowell NG, Erhardt EB, Hanson DT. *Plant, Cell Environ.* 2009; **32**: 796.
43. Barbour MM, Farquhar GD, Hanson DT, Bickford CP, Powers HH, McDowell NG. *Plant, Cell Environ.* 2007; **30**: 456.
44. Davenport DW, Wilcox BP, Allen BL. *Soil Sci. Soc. Am. J.* 1995; **59**: 1672.
45. Breshears DD. Structure and function of woodland mosaics: consequences of patch-scale heterogeneity and connectivity along the grassland-forest continuum. In *Western North American Juniperus Woodlands – A Dynamic Vegetation Type*, Van Auker OW (ed). Springer: New York, 2008; 58.
46. Butnor JR, Johnsen KH. *Eur. J. / Soil Sci.* 2004; **55**: 639.
47. Pendall E, Del Grosso S, et al. *Global Biogeochem. Cycles* 2003; **17**: 1046.
48. Schaeffer S, Anderson D, Burns S, Monson R, Sun J, Bowling D. *Agric. Forest Meteorol.* 2008; **148**: 592.
49. Barbour MM, McDowell NG, Tcherkez G, Bickford CP, Hanson DT. *Plant, Cell Environ.* 2007; **30**: 469.
50. Breecker D, Sharp ZD. *Rapid Commun. Mass Spectrom.* 2008; **22**: 449.
51. Breecker DO, Sharp ZD, McFadden LD. *Geol. Soc. Am. Bull.* 2009; **121**: 630.
52. Xu LK, Baldocchi DD, Tang JW. *Global Biogeochem. Cycles* 2004; **18**: GB4002.
53. Steinmann KTW, Siegwolf R, Saurer M, Korner C. *Oecologia* 2004; **141**: 489.
54. Nadelhoffer KJ, Fry B. *Soil Sci. Soc. Am. J.* 1988; **52**: 1633.
55. Wingate L, Seibt U, Maseyk K, Ogee J, Almeida P, Yakir D, Pereira JS, Mencuccini M. *Global Change Biol.* 2008; **14**: 2178.
56. Risk D, Kellman L. *Geophys. Res. Lett.* 2008; **35**: L02403.
57. Cuntz M, Ciais P, Hoffmann G, Allison CE, Francey RJ, Knorr W, Tans PP, White JWC, Levin I. *J. Geophys. Res. – Atmospheres* 2003; **108**: 4528.
58. Takle ES, Massman WJ, Brandle JR, Schmidt RA, Zhou X, Litvina IV, Garcia R, Doyle G, Rice CW. *Agric. Forest Meteorol.* 2004; **124**: 193.